*RNA* (2001), *7*:833–845. Cambridge University Press. Printed in the USA.


# A conserved pseudouridine modification in eukaryotic U2 snRNA induces a change in branch-site architecture

**MEREDITH I. NEWBY[1] and NANCY L. GREENBAUM[1,2]**

[1]Institute of Molecular Biophysics, Florida State University, Tallahassee, Florida 32306-4380, USA
[2]Department of Chemistry, Dittmer Laboratory of Chemistry, Florida State University, Tallahassee, Florida 32306-4390, USA

## ABSTRACT

**The removal of noncoding sequences (introns) from eukaryotic precursor mRNA is catalyzed by the spliceosome, a dynamic assembly involving specific and sequential RNA–RNA and RNA–protein interactions. An essential RNA–RNA pairing between the U2 small nuclear (sn)RNA and a complementary consensus sequence of the intron, called the branch site, results in positioning of the 2′OH of an unpaired intron adenosine residue to initiate nucleophilic attack in the first step of splicing. To understand the structural features that facilitate recognition and chemical activity of the branch site, duplexes representing the paired U2 snRNA and intron sequences from *Saccharomyces cerevisiae* were examined by solution NMR spectroscopy. Oligomers were synthesized with pseudouridine ($\psi$) at a conserved site on the U2 snRNA strand (opposite an A-A dinucleotide on the intron strand, one of which forms the branch site) and with uridine, the unmodified analog. Data from NMR spectra of nonexchangeable protons demonstrated A-form helical backbone geometry and continuous base stacking throughout the unmodified molecule. Incorporation of $\psi$ at the conserved position, however, was accompanied by marked deviation from helical parameters and an extrahelical orientation for the unpaired adenosine. Incorporation of $\psi$ also stabilized the branch-site interaction, contributing –0.7 kcal/mol to duplex $\Delta G^{\circ}_{37}$. These findings suggest that the presence of this conserved U2 snRNA pseudouridine induces a change in the structure and stability of the branch-site sequence, and imply that the extrahelical orientation of the branch-site adenosine may facilitate recognition of this base during splicing.**

**Keywords: branch site; NMR; pre-mRNA splicing; pseudouridine; RNA**

## INTRODUCTION

Precursor messenger (pre-m) RNA molecules of eukaryotes, as part of their maturation process, are spliced. Noncoding regions, or introns, are excised from nascent mRNA transcripts, and the flanking coding sequences, called exons, are ligated together. The splicing mechanism is catalyzed by the spliceosome, a dynamic assembly of five small nuclear (sn)RNAs (U1, U2, U4, U5, and U6) and numerous associated proteins (reviewed in Moore et al., 1993). In the first of two sequential transesterification reactions, the 2′OH of a specific adenosine within the intron, bulged out by pairing of the surrounding region with a complementary segment of the U2 snRNA, initiates nucleophilic attack on the phosphodiester linkage at the 5′ splice site (scheme shown in Fig. 1B). A 2′-5′ phosphodiester linkage is formed with this intron adenosine, forming the branch site.

The structural features of the eukaryotic branch-site region that promote its unique recognition and chemical activity are of great interest. Results of biochemical studies in which individual base functional groups were modified imply an extrahelical orientation of the adenine base (Query et al., 1996), although solution NMR structures of other RNAs with unpaired adenosines show the base intercalated between adjacent base pairs (e.g., Borer et al., 1995; Smith & Nikonowicz, 1998; Varani et al., 1999; see, however, Greenbaum et al., 1996). Of particular interest is the RNA that forms the binding site for phage GA coat protein, because of the sequence similarity it shares with the U2 snRNA–intron branch-site pairing. The solution structure of this RNA, characterized by an unpaired adenine that stacks within the helix (Smith & Nikonowicz, 1998), prompted us to ask whether the adenosine residue of the spliceosomal branch site is also stacked within the helix or adopts an extrahelical orientation.

Reprint requests to: Nancy L. Greenbaum, Department of Chemistry, Dittmer Laboratory of Chemistry, Florida State University, Tallahassee, Florida 32306-4390, USA; e-mail: nancyg@chem.fsu.edu.

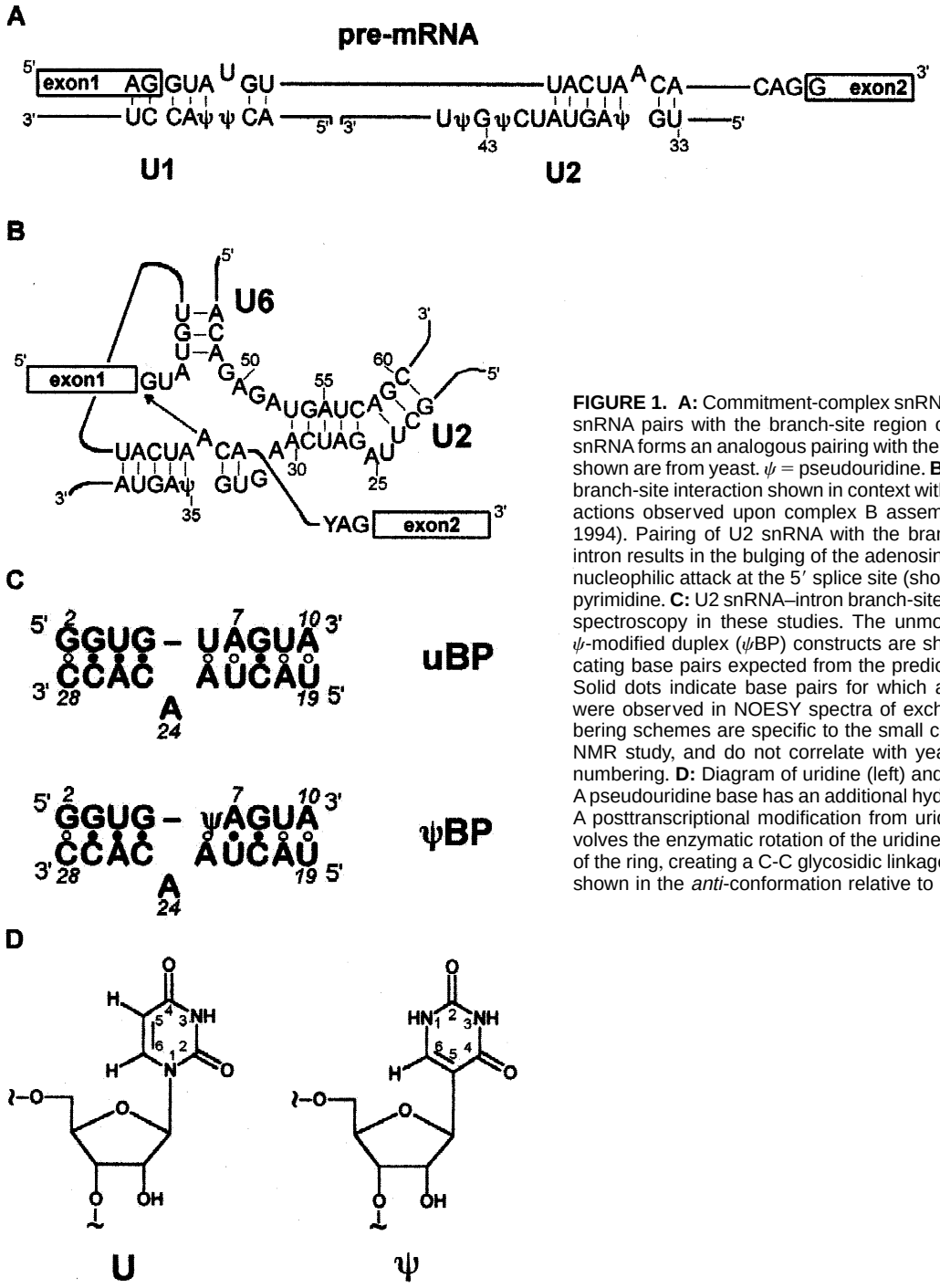


**FIGURE 1. A:** Commitment-complex snRNA–intron pairings. The U2 snRNA pairs with the branch-site region of the intron, and the U1 snRNA forms an analogous pairing with the 5′ splice site. Sequences shown are from yeast. $\psi$ = pseudouridine. **B:** Yeast U2 snRNA–intron branch-site interaction shown in context with nearby U6 snRNA interactions observed upon complex B assembly (Madhani & Guthrie, 1994). Pairing of U2 snRNA with the branch-site sequence of the intron results in the bulging of the adenosine residue responsible for nucleophilic attack at the 5′ splice site (shown by an arrow). Y = any pyrimidine. **C:** U2 snRNA–intron branch-site constructs used for NMR spectroscopy in these studies. The unmodified duplex (uBP) and $\psi$-modified duplex ($\psi$BP) constructs are shown with open dots indicating base pairs expected from the predicted secondary structure. Solid dots indicate base pairs for which associated imino protons were observed in NOESY spectra of exchangeable protons. Numbering schemes are specific to the small constructs synthesized for NMR study, and do not correlate with yeast U2 snRNA sequence numbering. **D:** Diagram of uridine (left) and pseudouridine ($\psi$; right). A pseudouridine base has an additional hydrogen bond donor (NH1). A posttranscriptional modification from uridine to pseudouridine involves the enzymatic rotation of the uridine base about the 3–6 axis of the ring, creating a C-C glycosidic linkage to the ribose. Bases are shown in the *anti*-conformation relative to their riboses.

Posttranscriptionally modified bases in snRNAs, including pseudouridines ($\psi$; a uridine base rotated to have a carbon–carbon glycosidic linkage and a second exposed imino group; Fig. 1D), have long been noted. Pseudouridines in tRNA molecules have been shown to stabilize existing helical structure by providing an additional hydrogen bond donor that participates in a water-mediated hydrogen bond with backbone phosphates (Arnez & Steitz, 1994; Davis, 1995). Molecular dynamics simulations support the premise that pseudouridines restrict the motion of neighboring bases (Auffinger & Westhof, 1998). Accordingly, the presence of pseudouridine residues has been associated with stabilization of short duplex RNAs and tRNA anticodon loops without perturbing local structure (Davis & Poulter, 1991; Hall & McLaughlin, 1991; Arnez & Steitz, 1994; Durant & Davis, 1999; Yarian et al., 1999).

Chemical mapping of U2 snRNA sequences of a number of species has documented many conserved pseudouridylation sites in U2 snRNA, particularly in the

5′ region of the sequence (Reddy & Busch, 1988; Patton et al., 1994; Gu et al., 1996; Massenet et al., 1999). Some of these modification sites have been implicated in proper assembly of the 17S U2 snRNP particle (Yu et al., 1998). In this study, we investigate the structural role of yeast U2 snRNA $\psi$35, a pseudouridine that pairs with the intron branch site directly opposite the A-A dinucleotide. Although functional studies have not identified a specific role for $\psi$35 in splicing (Wu & Manley, 1989; Yu et al., 1998; Behrens et al., 1993), the conservation of a pseudouridine in close proximity to the branch-site adenosine implies a structural role for this modified base. In this study, architectural features of the pseudouridine-modified and unmodified spliceosomal U2 snRNA–intron branch-site pairing of *Saccharomyces cerevisiae* were investigated using NMR spectroscopic methods, and stability was assessed by thermal denaturation assays. Our results demonstrate that the presence of the pseudouridine not only stabilizes the branch-site interaction as compared with an unmodified uridine at the same position, but changes the orientation of the bulged adenosine relative to the U2 snRNA–intron helix. These findings provide the first direct evidence of a pseudouridine inducing a structural change in RNA, and suggest that this pseudouridine may function to position the branch-site adenosine better for recognition and subsequent activity in splicing.

## RESULTS

### Assignment of exchangeable protons in branch-site constructs

Information about base pairing patterns for the unmodified duplex (uBP; Fig. 1C) was obtained from NMR spectra of exchangeable protons. One-dimensional spectra included four strong resonances in the 12.0–14.0 ppm region, indicative of imino protons involved in Watson–Crick base pairs (Table 1). End-fraying effects (Patel & Hilbers, 1975) precluded the observation of exchangeable proton resonances corresponding to imino protons at the termini or adjacent to unpaired nucleotides. The four imino resonances were assigned to protons in helical stem regions of the molecule (shown by the solid dots between base pairs in Fig. 1C) based upon NOEs in two-dimensional spectra, including imino–imino cross peaks and imino–amino cross peaks characteristic of A-U and G-C base pairs.

Similar NMR spectra were acquired using a duplex in which U6 was replaced by pseudouridine ($\psi$BP; Fig. 1C). Essentially the same imino–amino cross-peak patterns were observed in NOESY spectra of $\psi$BP as in spectra of uBP, with the addition of two new imino resonances. One of these new resonances was identified as U22 NH3 by its cross peak with A7 H2, and the other (at 10.55 ppm) was assigned to $\psi$6 NH1 based on an NOE to its own H6. Observation of the $\psi$6 NH1 resonance

**TABLE 1**. Chemical shifts for protons in branch-site constructs.

| | H1/H3 | | H6/H8 | | H5/H2 | | H1′ | | H2′ | | H3′ | |
|---|---|---|---|---|---|---|---|---|---|---|---|---|
| Base | uBP | $\psi$BP | uBP | $\psi$BP | uBP | $\psi$BP | uBP | $\psi$BP | uBP | $\psi$BP | uBP | $\psi$BP |
| G 2 | | | 8.07 | 8.08 | | | 5.81 | 5.80 | | 4.64 | | |
| G 3 | 13.37 | 13.40 | 7.47 | 7.47 | | | 5.87 | 5.88 | 4.47 | 4.46 | 4.55 | 4.52 |
| U 4 | 13.79 | 13.85 | 7.76 | 7.73 | 5.05 | 5.10 | 5.56 | 5.54 | **4.66**** | **4.44**** | 4.56 | 4.52 |
| G 5 | **13.48**** | **13.58**** | 7.67 | 7.72 | | | 5.81 | 5.80 | **4.46**** | **4.65**** | 4.51 | 4.45 |
| $\psi$/U6 | | 10.55† | **7.66**** | **7.05**** | 5.16 | | **5.50**** | **4.42**** | 4.42 | 4.43 | **4.53*** | **4.60*** |
| A 7 | | | 8.09 | 8.04 | **6.96**** | **6.84**** | 5.83 | 5.77 | 4.63 | 4.57 | 4.64 | 4.68 |
| G 8 | 12.60 | 12.65 | 7.25 | 7.23 | | | **5.27**** | **5.38**** | 4.26 | 4.25 | 4.36 | 4.35 |
| U 9 | | | 7.59 | 7.60 | 5.07 | 5.05 | 5.46 | 5.45 | 4.25 | 4.22 | 4.49 | 4.46 |
| A 10 | | | 8.08 | 8.11 | 7.38 | 7.41 | 6.05 | 6.03 | 4.15 | 4.12 | 4.28 | 4.26 |
| U 19 | | | 8.08 | 8.09 | 5.83 | 5.82 | 5.54 | 5.58 | 4.60 | 4.57 | 4.33 | 4.31 |
| A 20 | | | 8.36 | 8.39 | 7.37 | 7.43 | 6.05 | 6.02 | 4.64 | 4.64 | 4.55 | 4.54 |
| C 21 | | | 7.57 | 7.59 | 5.25 | 5.27 | 5.39 | 5.38 | 4.20 | 4.16 | 4.40 | 4.37 |
| U 22 | | 13.11 | 7.80 | 7.78 | 5.40 | 5.37 | 5.69 | 5.69 | 4.28 | 4.27 | 4.60 | 4.60 |
| A 23 | | | **8.19*** | **8.26*** | **7.42**** | **7.64**** | 6.00 | 6.04 | 4.56 | 4.56 | **4.54*** | **4.36*** |
| A 24 | | | **8.16*** | **8.23*** | **7.65**** | **7.85**** | **5.84*** | **5.91*** | 4.59 | 4.62 | **4.64**** | **4.37**** |
| C 25 | | | **7.45**** | **7.55**** | 5.15 | 5.09 | 5.36 | 5.40 | 4.36 | 4.36 | 4.44 | 4.43 |
| A 26 | | | 8.10 | 8.10 | 7.48 | 7.48 | 5.93 | 5.92 | 4.55 | 4.53 | 4.50 | 4.33 |
| C 27 | | | 7.51 | 7.55 | 5.21 | 5.16 | 5.39 | 5.40 | 4.13 | 4.11 | 4.37 | 4.34 |
| C 28 | | | 7.61 | 7.64 | 5.44 | 5.41 | 5.66 | 5.66 | 4.02 | 3.98 | 4.15 | 4.12 |

Bold numbers represent significant differences between chemical shifts for uBP and $\psi$BP. Due to conformational flexibility of the termini, the H2′ and H3′ proton chemical shifts for 5′ bases were difficult to assign; therefore the somewhat ambiguous shifts for G2 have been left blank.

*: $0.07 \leq |(uBP_{ppm} - \psi BP_{ppm})| < 0.1$.

**: $|(uBP_{ppm} - \psi BP_{ppm})| \geq 0.1$.

†$\psi$6 NH1 proton.

implies that the proton is protected from rapid exchange, possibly by involvement in a non-Watson–Crick hydrogen bond (Hall & McLaughlin, 1992).

### Assignments of nonexchangeable protons of branch-site constructs

Assignment of aromatic (H8/H6/AH2) and ribose H1′ proton resonances in unmodified and $\psi$-modified branch-site constructs was achieved by standard strategies (Wijmenga et al., 1993) from two-dimensional homonuclear spectra (Table 1). Pyrimidine aromatic resonances were identified from H6-H5 cross peaks observed in TOCSY spectra. The assignment process was assisted by sequential base-H1′ NOE connectivities that were continuous throughout the bulged regions of each duplex (Fig. 2A,B). Resonance positions of corresponding aromatic and anomeric protons in the helical stem regions of the two duplexes were essentially identical. A number of corresponding proton resonances in both strands of the bulged region, however, displayed differences, suggesting conformational variance between the two constructs (Table 1). Specifically, the A7 H2 resonance of $\psi$BP displayed an upfield shift of 0.12 ppm, and G8 H1′, C25 H6, A23 H2, A23 H8, A24 H8, and A24 H1′ resonances shifted downfield by 0.07–0.22 ppm compared with their counterparts in uBP. Upfield chemical shifts for $\psi$6 H6 and H1′ protons were typical of values seen previously for pseudouridines (Davis, 1995). To assign A24 H2, one-dimensional traces of NOESY spectra of both constructs were compared to identify any aromatic resonances that did not exhibit any NOEs at 350 ms mixing times and shorter. The A24 H2 resonance appeared as a strong, slightly broadened peak at 7.85 ppm in one-dimensional spectra of $\psi$BP, and was the only resonance in the aromatic region that did not exhibit cross peaks in two-dimensional NOESY spectra. A much diminished resonance is also seen at this position in spectra of uBP, suggesting that either a very small percentage of the unmodified construct maintains an extrahelical A24, or that uBP is dynamic, and a small portion of the time, the unpaired adenosine is in a looped-out conformation.

### Conformational features of branch-site duplexes determined from NOE patterns

Spectra of uBP and $\psi$BP constructs exhibited NOEs typical of A-type helical geometry for stem regions flanking the unpaired adenosine, including those involving adenosine H2 protons. Because AH2 protons in A-form helices display characteristic NOEs to sequential $H1'_{i+1}$ and cross-strand $H1'_{i-1}$ ribose protons, deviation from helical parameters is reflected in alteration of these patterns. We therefore focused on NOE interactions involving H2 protons of A7, A23, and A24 to gather structural information about bulged region conformations of $\psi$BP and uBP.

Several NOEs observed in NOESY spectra of uBP defined the intrahelical orientation of bases of the branch-site region in the unmodified construct (Fig. 2A; Tables 2 and 3). For example, a sequential NOE between A23 H2 and A24 H1′ and a cross-strand NOE between A23 H2 and A7 H1′ were consistent with a stacked conformation for A23. The intrahelical position of A24 (the branch-site adenosine) was verified by a sequential NOE between A24 H2 and C25 H1′ NOE, a cross-strand $i \rightarrow i-1$ NOE between A24 H2 and U6 H1′, and a long-range cross-strand $i \rightarrow i-2$ NOE between A24 H2 and A7 H1′. Overall, NOE patterns exhibited by AH2 protons in the bulged region of uBP were essentially identical to those observed in the flanking helical stems of the molecule.

In contrast, NOE patterns involving AH2 protons in the corresponding region of $\psi$BP were inconsistent with A-form helical geometry, and implied an extrahelical orientation of the unpaired adenosine. In particular, A7H2 of $\psi$BP did not exhibit the NOEs to A23 H1′ or A24 H1′ protons that were observed in equivalent spectra for uBP (Table 2). Evidence that A23 was stacked in the helix was provided by NOEs between its H2 and A7 H1′, $\psi$6 H1′, and C25 H1′, but the absence of any NOEs involving A24 H2 suggests an extrahelical position for this base. The observation of an unusual sequential $i \rightarrow i+2$ NOE between A23 H2 and C25 H1′ strengthened this conclusion. Unambiguous assignment of this NOE was verified in NOESY spectra with very long ($>$1.5 s) mixing times (allowing the partially overlapped H5-H6 cross peak to disappear). An NOE between A23 H2 and $\psi$6 H1′, as well as the absence of an NOE between A7 H2-A23 H1′, suggested that A23 was further from the U22-A7 base pair, and closer to C25 than in the unmodified duplex (Fig. 3).

### Conformation of riboses and $^{31}$P studies in branch-site constructs

Values for ribose H1′-H2′ scalar couplings were measured in DQF-COSY spectra of uBP and $\psi$BP (Table 4). Riboses in the unmodified molecule, except for those at the termini, exhibited very small couplings ($<$2–3 Hz) typical of C3′-*endo* character and A-form helical geometry. Spectra for $\psi$BP, however, exhibited a $J_{H1'\text{-}H2'}$ coupling of approximately 7.3 Hz for the unpaired adenosine, A24, indicative of C2′-*endo* conformation for this sugar. The H1′-H2′ scalar coupling of approximately 6 Hz for A23 and 5.6 Hz for U22 indicated an alternative *exo* sugar conformer or a ribose in equilibrium between C3′- and C2′-*endo* puckers (Altona, 1982). The presence of these alternative sugar conformers in the modified branch-site vicinity indicated a deviation from A-form geometry in $\psi$BP. In contrast, all nonterminal

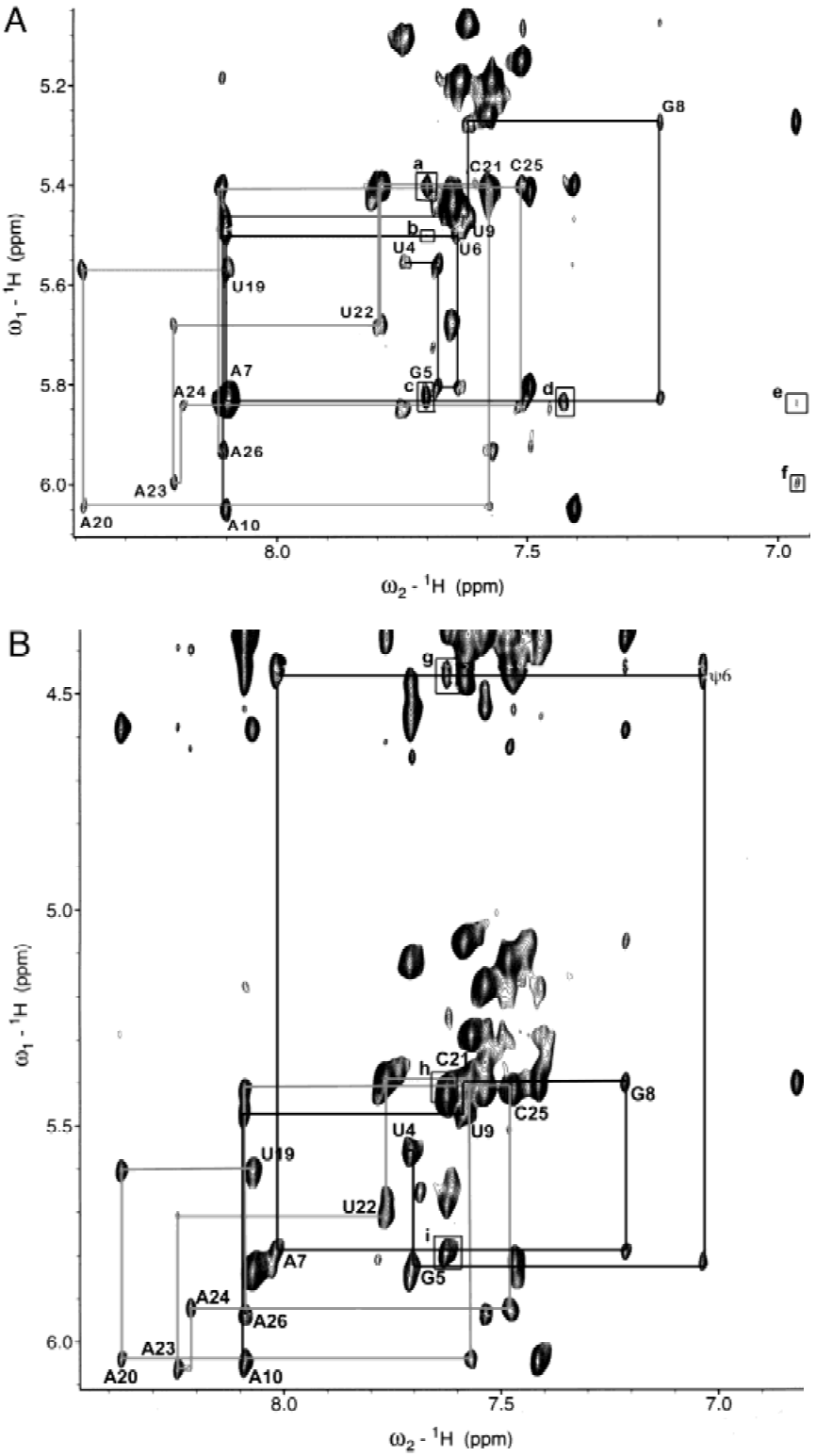


**FIGURE 2.** Aromatic-anomeric regions of two-dimensional NOESY spectra acquired for uBP (**A**) and $\psi$BP (**B**) branch-site constructs with a mixing time of 350 ms. Sample concentrations were approximately 0.8 mM and 1.2 mM, respectively. The spectra were acquired in 10 mM sodium phosphate, 0.1 mM EDTA, 50 mM NaCl (pH 6.4) in 99.96% $^2H_2O$ at 20 °C. Connectivities are shown between sequential base H6/H8 and H1′ protons. The U2 snRNA strand is shown in black (U4 through A10), and the intron strand is shown in gray (U19 through A26). Bases are numbered at the intramolecular H6/H8-H1′ cross peak. NOEs involving AH2 protons in the branch-site region are indicated by black boxes: A24 H2-A25 H1′ (a), A24 H2-U6 H1′ (b), A24 H2-A7 H1′ (c), A23 H2-C25 H1′ and A23 H2-A24 H1′ (d), A7 H2-A24 H1′ (e), A7 H2-A23 H1′ (f), A23 H2-$\psi$6 H1′ (g), A23 H2-C25 H1′ (h), and A23 H2-A7H1′ (i).

**TABLE 2**. Comparison of long-range and cross-strand intermolecular NOEs in the uBP and ψBP bulged-base region, observed in spectra collected with a mixing time of 350 ms.

| uBP | ψBP |
|---|---|
| A7H2-A23H2 | |
| A7H2-A23H1′ | |
| A7H2-A24H1′ | |
| A23H2-A7H1′ | A23H2-A7H1′ |
| A23H2-A24H1′ | |
| | A23H2-ψ6H1′ |
| | A23H2-C25H1′ |
| A24H2-A7H1′ | |
| A24H2-U6H1′ | |
| A24H2-C25H1′ | |
| U4NH3-A26H2 | U4NH3-A26H2 |
| G5NH1-C25NH2 | G5NH1-C25NH2 |
| | U22NH3-A7H2 |

**TABLE 3**. Comparison of short-range and sequential intermolecular NOEs in the uBP and ψBP bulged-base region, observed in spectra collected with a mixing time of 350 ms.

| uBP | ψBP |
|---|---|
| U4H1′-G5H8 | U4H1′-G5H8 |
| G5H1′-U4H2′ | G5H1′-U4H2′ |
| G5H1′-U6H6 | G5H1′-ψ6H6 |
| G5H1′-U6H5 | |
| U6H1′-G5H2′ | |
| U6H1′-A7H8 | ψ6H1′-A7H8 |
| C25H6-A26H8 | ψ6H1′-A7H1′ |
| U22H1′-A23H8 | U22H1′-A23H8 |
| A23H1′-A24H8 | A23H1′-A24H8 |
| | A23H1′-U22H2′ |
| U4H3′-G5H8 | A23H1′-A24H1′ |
| A24H1′-C25H6 | A24H1′-C25H6 |
| A24H1′-C25H5 | A24H1′-C25H5 |
| A24H1′-A23H2′ | A24H1′-A23H2′ |
| C25H1′-A26H8 | C25H1′-A26H8 |
| C25H1′-A24H2′ | |
| | C25H1′-A24H1′ |
| U4H2′-G5H8 | U4H2′-G5H8 |
| U4H3′-G5H8 | H4H3′-G5H8 |
| G5H2′-U6H5 | |
| G5H2′-U6H6 | G5H2′-ψ6H6 |
| G5H3′-U6H5 | |
| G5H3′-U6H6 | G5H3′-ψ6H6 |
| U6H2′-A7H8 | ψ6H2′-A7H8 |
| U6H3′-A7H8 | ψ6H3′-A7H8 |
| U22H2′-A23H8 | U22H2′-A23H8 |
| U22H3′-A23H8 | U22H3′-A23H8 |
| A23H2′-A24H8 | A23H2′-A24H8 |
| A23H2′-A24H8 | A23H2′-A24H8 |
| A24H2′-C25H6 | A24H2′-C25H6 |
| A24H3′-C25H6 | A24H3′-C25H6 |
| | A24H2′-C25H5 |
| C25H2′-A26H8 | C25H2′-A26H8 |
| C25H2′-A26H8 | C25H2′-A26H8 |
| | G5H8-ψ6H6 |
| U6H6-A7H8 | ψ6H6-A7H8 |
| U22H6-A23H8 | U22H6-A23H8 |
| | A23H8-A24H8 |
| | A24H8-C25H6 |
| | C25H6-A26H8 |
| U4NH3-G5NH1 | U4NH3-G5NH1 |
| U4NH3-A26NH2 | U4NH3-A26NH2 |

riboses in the unmodified duplex had C3′-*endo* sugar conformers, as expected for A-form geometry.

Phosphorous NMR studies were conducted to assess differences in backbone conformation between the modified and unmodified constructs. Proton decoupled one-dimensional NMR spectra were collected on uBP, ψBP, and a 9-bp duplex without the bulged adenosine (ubBP), and were referenced to an external standard of 85% phosphoric acid. Phosphorous resonances for both uBP and ubBP all fell within a narrow range typical of an A-form helix, from 0.0 to −1.0 ppm, and were heavily overlapped. Resonances for ψBP, however, spanned a somewhat greater range, from +0.1 to −1.2 ppm. The severe overlap in all spectra (one- and two-dimensional) precluded further assessment by $^{1}H$-$^{31}P$ correlation spectroscopy. Although definitive conclusions cannot be drawn from these phosphorous data alone, taken together with data for H1′-H2′ J-coupling measurements, we tentatively conclude that the backbone deviates from standard A-form geometry in ψBP.

### Effects of pH and ion concentration on branch-site constructs

The effects of cobalt (III) hexamine and magnesium chloride were investigated on the uBP and ψBP branch-site constructs at 20 °C. No change in NOESY spectra of nonexchangeable protons of either duplex was observed upon addition of 5 mM Co(III) hexamine. In particular, there was no indication of an NOE between a base imino proton and an amino of the ion complex that would be expected for specific binding in the major groove (Kieft & Tinoco, 1997). Similarly, no changes were observed in NOESY spectra of either duplex upon addition of $MgCl_2$. Very slight broadening and shifting of nonexchangeable resonances was observed in NOESY spectra of both duplexes, and was attributed to nonspecific binding of magnesium cations to backbone phosphates.

The effects of pH on branch-site structure were difficult to assess because the short duplexes used in this study denatured at pH above 7.5 or below 5.0. However, within that range, no new peaks were observed upon increasing or decreasing the pH from the optimal pH (6.4). Interestingly, at low pH (<5.5), the last remaining imino resonance is that of ψ6NH1.

### Thermal denaturation of branch-site duplexes

The stability of the duplexes was evaluated by measurement of melting transitions. Predicted melting temperatures ($T_m$) calculated from nearest-neighbor ap-

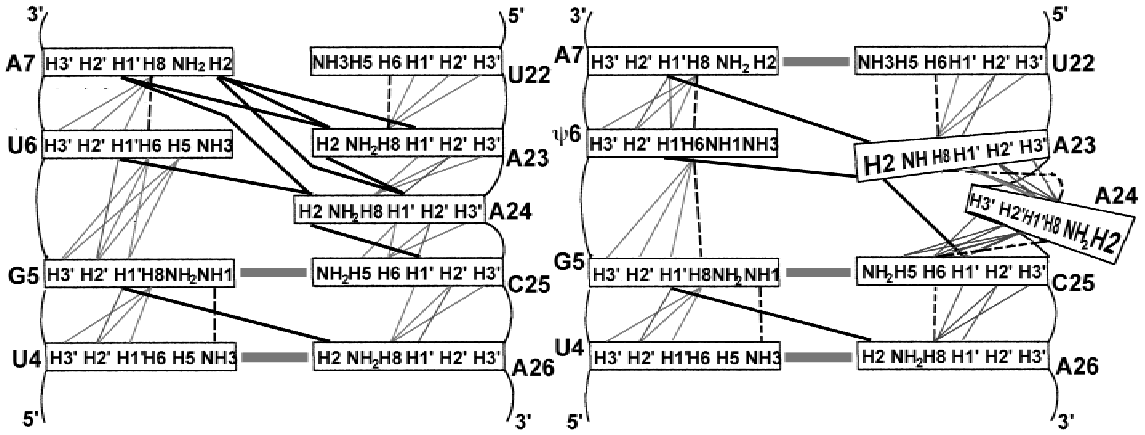


**FIGURE 3.** Schematic NOE diagrams of the bulged regions of uBP and $\psi$BP constructs. Lines drawn indicate intermolecular NOEs between nonexchangeable protons observed in NOESY spectra with mixing times of 350 ms. Thick gray lines between bases on opposing strands indicate base pairs verified by NOEs in spectra of exchangeable protons. Thin gray lines represent sequential H6/H8-H1′, -H2′, and -H3′ and H5-H1′, -H2′, and -H3′ interactions, and also H1′-H2′ intermolecular NOEs. Sequential H6/H8-H6/H8 NOEs observed are shown by dashed black lines, and solid black lines signify NOEs involving adenosine H2 protons.

proximation of free energy parameters (Freier et al., 1986) were compared with experimental values. The predicted $T_m$ for a 9-bp duplex of the same sequence but without the unpaired base (ubBP) sequence was 53.9 °C. Introduction of a single bulged adenosine residue into the sequence decreased the predicted $T_m$ to 39.9 °C. No values were available for calculation of $T_m$ for the corresponding sequence with the modified base. Experimental melting transitions observed for all duplexes, measured by changes in absorbance at 260 nm upon heating, were characterized by sigmoidal curves indicative of cooperative two-state transitions (Saenger, 1984; Puglisi & Tinoco, 1989). Calculated $T_m$ and free energies of formation (ΔG°) derived from van't Hoff analysis of denaturation profiles, shown in Table 5, were consistent with the predicted values for the unmodified duplexes. Substitution of pseudouridine for an unmodified uridine resulted in a pairing approximately −0.7 kcal/mol more stable than the unmodified duplex (uBP). In contrast, incorporation of a deoxypseudouridine (d$\psi$BP) into the sequence in place of pseudouridine destabilized the interaction by 0.7 kcal/mol over that of the unmodified duplex. We noted that the denaturation profile of uBP was less sigmoidal than the profile for either d$\psi$BP or $\psi$BP, that is, presence of a modified base induced a more cooperative transition from duplex to single-stranded species (data not shown).

## DISCUSSION

Modification sites are often highly conserved throughout evolution in both single- and double-stranded regions of RNA (Foster et al., 2000). Pseudouridine, the most common posttranscriptionally modified residue in RNA, has been identified in transfer, ribosomal, and small nuclear RNAs, where it contributes added stability to RNA architectural elements. The N1 imino group of pseudouridine provides an additional substituent for recognition and an additional hydrogen bond donor. The peptidyl transferase center of rRNA contains highly conserved pseudouridine modifications that provide the region with a high level of specificity for catalytic interaction with its substrate (Bakin et al., 1994).

**TABLE 4.** $J_{H1'-H2'}$ couplings measured from DQF-COSY spectra of $\psi$BP.

| Ribose | $J_{H1'-H2'}$ (Hz) |
|---|---|
| A 10 | 8.0 ± 0.2 |
| U 22 | 5.6 ± 0.2 |
| A 23 | 6.0 ± 0.2 |
| A 24 | 7.3 ± 0.2 |
| C 28 | 8.0 ± 0.2 |

**TABLE 5.** Melting transitions measured by changes in absorbance at 260 nm between 10 °C and 80 °C.

| Branch-site construct | Melting temperature (°C) | $\Delta G^\circ_{37}$ (kcal/mol) |
|---|---|---|
| ubBP | 49.1 | −10.8 |
| uBP | 37.2 | −8.8 |
| d$\psi$BP | 34.7 | −8.1 |
| $\psi$BP | 41.8 | −9.5 |

The sample was comprised of approximately 4.5 $\mu$M RNA duplex in 10 mM sodium phosphate (pH 6.4), 0.1 mM EDTA, 1 M NaCl. Melting temperatures were identified at $\alpha = 0.5$ on a least linear-squares fit line of the melting transition plotted as fraction melted ($\alpha$) versus temperature. Error in calculated melting temperatures is less than 0.3 °C, and error in $\Delta G^\circ_{37}$ is ±5%.

Recent chemical mapping of yeast U2 snRNA has identified many posttranscriptional uridine-to-pseudouridine modifications in the sequence, including $\psi$35, a pseudouridine in the region of U2 snRNA that pairs with the intron branch site (Massenet et al., 1999). The fact that this modification has been identified at the same location in all eukaryotic systems examined to date, from yeast to mammals (Reddy & Busch, 1988; Patton et al., 1994; Gu et al., 1996; Yu et al., 1998; Massenet et al., 1999), lends credence to the hypothesis that it maintains an important role in branch-site structure and activity. The data presented here provide the first evidence, to our knowledge, of a pseudouridine inducing a local conformational change in an RNA molecule.

### Structural features of the branch site in the unmodified sequence

NOE patterns and proton correlation data throughout the uBP construct were found to be consistent with typical A-form helical geometry, and cross-strand NOEs involving adenine H2 protons were consistent with an intrahelical position for both adenosine residues in the branch-site region (Fig. 3). We compared our data with those of Smith & Nikonowicz (1998) for the folded RNA sequence recognized by the phage GA coat protein, which contains an unpaired adenosine in a context similar to the yeast U2 snRNA–intron pairing (the only difference is a G-C base pair immediately 3′ to the unpaired A instead of a C-G base pair in the branch site). The NOE interactions that constrained the extra adenosine of the phage RNA to a position intercalated within the helix (Smith & Nikonowicz, 1998) were also seen in spectra of uBP. We therefore conclude that a similar stacking of the adenosine residues is likely to occur in the unmodified U2 snRNA–intron helix as in the RNA recognized by the phage GA coat protein. In contrast with spectra of $\psi$BP, where an NOE was observed between G5H8 and $\psi$6H6, no analogous NOE is seen between G5H8 and U6H6 in uBP spectra. The absence of this NOE is consistent with a larger spacing between these sequential bases than is expected for A-type geometry, and presumably allows for the stacked position of A24 (e.g., as reported by Thiviyanathan et al., 2000, for a model RNA duplex featuring an intercalated unpaired adenosine).

If both A24 and A23 are stacked within the U2 snRNA–intron helix, which of these bases, or do both, participate in a base pair with the opposing uridine (U6)? Although no exchangeable proton NOEs providing direct evidence of base pairing in this region were observed, a cross-strand $i \rightarrow i - 2$ NOE between A24 H2 and A7 H1′ implied that A24 is close enough to form a hydrogen bond with U6. Smith and Nikonowicz (1998) identified an (A-A)-U motif involving a protonated adenine in their structural model; similar NOE patterns in spectra of the unmodified U2 snRNA–intron duplex suggest that a similar motif may also occur here, although heteronuclear experiments on an isotopically labeled sample would be required to confirm it.

### Evidence for an extrahelical adenosine in the modified duplex

NOEs involving protons in the bulge region of the $\psi$BP duplex, particularly those involving H2 protons, were very different from those of the unmodified sequence, pointing out that modification of uridine $\rightarrow$ pseudouridine in this sequence results in a marked conformational change in the bulged region (Tables 2 and 3). Compelling evidence that A24 was extruded from the helix came from NOE cross peaks in this region (Fig. 3) and the complete lack of any NOEs involving A24 H2, and an $i \rightarrow i + 2$ NOE between the flanking bases. Although the absence of NOEs could be explained by conformational averaging due to motion of the base on the NMR time scale, we do not favor this explanation because the H8 resonance line width of A24 is relatively narrow, and the A24 H2 resonance is only slightly broad. In addition to NOE data supporting our assignment of A24 H2 and A23 H2 resonances, evidence from biochemical studies suggest that A24 is extrahelical. The functional groups on the branch-site adenosine (corresponding to A24 in our constructs) that are recognized, and therefore accessible during spliceosome assembly (Query et al., 1996), are consistent with our structural evidence of the extrahelical A24. Other sequences in which NOEs between residues flanking bulged bases have been used to define their extrahelical position include the TAR-argininamide complex (in which an $i \rightarrow i + 4$ NOE was observed; Puglisi et al., 1992) and the splice donor site of the SL1 RNA sequence from *Caenorhabditis elegans* (Greenbaum et al., 1995, 1996).

In addition to adenosine H2 NOE patterns (Table 2), other NOE data support the premise that the branch-site adenosine adopts an extrahelical position in $\psi$BP, besides the difference in adenosine H2 NOE patterns (Table 3). Base–base NOEs involving aromatic protons of A23, A24, and C25 present in $\psi$BP spectra, but not in uBP spectra (Table 3), suggest that these protons either are nearer in the modified construct, or that base motion is more restricted in the more thermally stable $\psi$BP duplex. There is no H5 in a pseudouridine (Fig. 1D), limiting the number of nonexchangeable NOEs between G5 and $\psi$6 (with respect to the number observed for equivalent bases in uBP).

All resonance shifts of 0.07 ppm or greater occur only in the bulged-base region of the branch-site duplex, that is, between U4-G8 and A23-C25 (Table 1). A general trend in the bulge region differences between the two constructs is the small downfield shifting of A23H8, A24H8, C25H6, A23H2, A24H2, and A24H1′ on the intron strand upon incorporation of the pseudouridine, suggesting a more exposed environment for

these protons. The upfield shift of A7H2 suggests a more protected environment for that proton, corroborated by the fact that we observe an NOE between U22 NH1 and A7H2 in exchangeable proton spectra of $\psi$BP, and not uBP. The upfield shifts for the H1′ of $\psi$6 are typical for a pseudouridine (Davis, 1995); therefore, no structural conclusions can be drawn from the widely different shifts for this proton between the two constructs.

The relative weakness of the sequential NOE between A23H8 and U22 H1′, compared with its counterpart in uBP spectra, and the absence of an NOE between A7H2 and A23 H1′ suggests a tilting of A23 toward C25 in $\psi$BP (schematically shown in Fig. 3).

### Increased thermal stability of the pseudouridine-modified branch-site construct

Thermal denaturation studies of branch-site duplex constructs demonstrated added stability upon substitution of uridine with pseudouridine at the conserved position in the U2 sequence (Table 5). The decrease in $\Delta G^{\circ}_{37}$ of 0.7 kcal/mol in $\psi$BP compared with its unmodified counterpart was comparable to free energy differences measured for tRNA anticodon stem loops with pseudouridine incorporation at the closing base pair of the loop (Durant & Davis, 1999; Yarian et al., 1999). A similar decrease was noted by Hall and McLaughlin (1991) upon substitution of two side-by-side uridine residues with pseudouridine in a self-complementary 11-nt duplex. Although the sequences varied in these experiments, the data suggest that increased stability is a common feature of pseudouridine, probably induced by the additional hydrogen bonding in each case. Incorporation of the pseudouridine also resulted in a more cooperative melting transition than observed in the unmodified duplex, which, combined with the slower exchange of protons observed in the unpaired region of the $\psi$BP duplex, suggests that stacking and additional hydrogen bonding in the bulged region contributes to the stability of the duplex. In contrast, incorporation of a deoxypseudouridine residue at the same location increased the free energy of formation ($\Delta G^{\circ}_{37}$) of the branch-site interaction by 0.7 kcal/mol relative to uBP (and by 1.4 kcal/mol with respect to $\psi$BP). This finding is in accord with experimental data of Bevilaqua and Turner (1991) that demonstrated unfavorable $\Delta G^{\circ}_{37}$ contributions to RNA duplex formation by deoxyriboses.

Davis (1995) observed that the values of $J_{H1'\text{-}H2'}$ couplings measured for riboses in a short single-stranded oligo decreased when a pseudouridine residue was substituted for uridine in a given sequence. Applying the generally held view that the thermal stability of RNA helices is related to A-form helical parameters (Lee & Tinoco, 1977), Davis attributed the greater propensity toward C3′-*endo* ribose conformation to increased base stacking. This conclusion was further supported by circular dichroism experiments in which incorporation of a pseudouridine residue caused increased temperature dependence of ellipticity at 270 nm (Davis, 1995). In our experiments, however, $J_{H1'\text{-}H2'}$ couplings indicative of non-C3′-*endo* conformation were measured for the riboses of residues opposing the pseudouridine in $\psi$BP (U22, A23, and A24), and one-dimensional phosphorous studies showed a 30% broader chemical shift range for $\psi$BP compared with an analogous unbulged helix (ubBP). In contrast, all nonterminal riboses of uBP had very small couplings characteristic of a C3′-*endo* pucker, and one-dimensional phosphorous NMR data suggest that the backbone conformation of uBP differs very little from an unbulged A-form helix. We consider it very interesting, therefore, that the presence of the pseudouridine in $\psi$BP resulted in a deviation from helical parameters, but that this duplex also exhibits greater thermal stability than uBP, the duplex that appears to maintain A-form geometry. Although the chemical shift of individual phosphorous resonances is not a singularly reliable predictor of specific perturbations in backbone geometry (Nikonowicz & Gorenstein, 1990), we speculate that the increased stability of $\psi$BP is the result of stabilizing interactions involving the pseudouridine NH1 and unusual backbone conformation in the bulged region. The increased number of imino proton resonances and NOESY cross peaks assigned to the bulged region of $\psi$BP as compared with the equivalent region of uBP is consistent with a more structured bulged region environment in the modified molecule.

### Bulged adenosines and pseudouridines as structural features

The propensity for extrahelical conformations of unpaired adenosines in crystallized molecules as a result of end-to-end stacking and intermolecular interactions has been well documented (Hermann & Patel, 2000). Very few NMR-derived structures depict single-bulged adenosines in extrahelical base conformations. In solution, it is simply less energetically favorable to expose a base to solvent than to stack one within a helix (Thiviyanathan et al., 2000). It is therefore intriguing that a U $\rightarrow \psi$ modification in a base pair adjacent to the unpaired adenosine in the branch-site duplex is sufficient to shift the energetically favored conformation of the base from a stacked to an extrahelical position. Pseudouridines in other contexts assume a stabilizing role in RNA structure. Water-mediated hydrogen bonds between pseudouridine N1 imino protons and phosphate oxygen atoms, predicted by molecular dynamics simulations (Auffinger & Westhof, 1998), and observed in tRNA anticodon loop structures determined by NMR (Durant & Davis, 1999) and X-ray crystallographic methods (Arnez & Stietz, 1994), contribute to the stability of RNA molecules (Hall & McLaughlin, 1991, 1992; Davis, 1995).

Pseudouridines are also abundant in all of the snRNAs, although their specific roles are not known. A study by Hall and McLaughlin (1991) of a duplex representing the pairing of human U1 snRNA and the intron 5′ splice site suggests that two side-by-side pseudouridines in the U1 snRNA sequence (Fig. 1A) do not alter helix structure, but together stabilize duplex formation by approximately 0.4–0.5 kcal/mol. Although the duplex in this study contained two pseudouridines, there were no mismatched base pairs or bulged bases (the human intron sequence has two adenosines that oppose the pseudouridines in the U1 snRNA sequence). In contrast, the single pseudouridine residue in the U2 snRNA–intron duplex apparently forms a base pair with an adenosine that is immediately adjacent to an unpaired adenosine, and alone contributes approximately 0.7 kcal/mol to duplex stability. If the pseudouridines in the U1 snRNA–intron duplex form water-mediated hydrogen bonds with phosphate oxygen atoms, as has been suggested (Hall & McLaughlin, 1992; Arnez & Steitz, 1994; Davis, 1995), we might expect the added stabilization to correlate with the number of pseudouridines. The large decrease in $\Delta G^{\circ}_{37}$ observed upon incorporation of pseudouridine at the conserved site in the U2 snRNA–intron construct implies that $\psi$35 may have a different structural role than the pseudouridines in the U1 snRNA–intron helix. In the study by Hall and McLaughlin (1991), disappearance of pseudouridine NH1 resonances upon increasing temperature was concurrent with the disappearance of all other imino resonances in the duplex. In contrast, the $\psi$NH1 resonance of $\psi$BP is the last imino resonance to disappear upon denaturation of the duplex at low pH. These results indicate that $\psi$NH1, presumably located in the major groove of the helix, is more stable upon denaturation than the Watson–Crick base-paired imino protons.

Crystal data show that a single extrahelical adenosine widens the major groove of an RNA helix (Portman et al., 1996). We propose that the extrahelical adenosine in $\psi$BP widens the major groove of the helix, thereby increasing the number of favorable water contacts and compensating for the energy cost of extruding the base into solvent. Although we see evidence for a widened major groove, we observe no NOEs from imino protons to a specific amine resonance that could be attributed to a bound cobalt (III) hexamine (Kieft & Tinoco, 1997), nor do we see any indication of magnesium binding (as did Hall & McLaughlin, 1991). We therefore conclude that no metal is required to stabilize the extrahelical conformation of the branch-site adenosine in the presence of $\psi$35.

### Conservation of $\psi$35

In spite of the documented conservation of $\psi$35 and its apparent role in branch-site structure (these studies), functional studies have not found that this specific modification is essential for splicing. Mutational studies of the U2 snRNA–intron pairing by Wu and Manley (1989) demonstrated that branch-site selection involves the base pairing of U2 snRNA to a consensus sequence of the intron. These authors found, however, that other base pairs can substitute for the wild type, albeit not as efficiently. Another study by Yu and colleagues (1998) found that the modifications in the first 27 nt of *Xenopus* U2 snRNA were the only sites critical for snRNP assembly, likely because they mediate the specificity of RNA–protein interactions; nine U2-specific proteins are known to bind with low affinity the first stem-loop of free U2-snRNA (Behrens et al., 1993).

The branch-site consensus sequence is poorly conserved among eukaryotes (Wu & Manley, 1989). In group II introns, not only are the base pairs flanking the bulged adenosine poorly conserved among these self-splicing introns, but the first step of splicing apparently occurs if the branch-site adenosine is involved in a Watson–Crick base pair (Chu et al., 1998). This finding may diminish the importance of a pseudouridine residue in the spliceosome that facilitates bulging of this residue. However, there are many documented differences between branch-site recognition in group II introns and spliceosomes. Specifically, the N6 of the branch-site adenosine is the major determinant in recognition in group II introns (Liu et al., 1997) whereas the N1 is the most important substituent in spliceosomes (Query et al., 1996). Also, a cytosine can be tolerated at the spliceosome branch site, but it is not acceptable as a branch point in group II introns. These differences suggest a different mode of recognition for the branch site in spliceosomes and group II introns.

In spite of the observation that a certain amount of variability is tolerated in the identity of complementary base pairs adjacent to the branch site, the modification of U $\rightarrow \psi$ we investigate in this study is highly conserved among species. Mutations of yeast U2 snRNA at position 35 result in decreased splicing efficiency (McPheeters & Abelson, 1992), and we have provided evidence that its presence induces a change in branch-site structure. Whether this structural change is related to recognition of the branch site, or is related to other processes in splicing awaits further studies. We speculate that the U $\rightarrow \psi$ modification at position 35 adds specificity to a recognition event, such as that of the branch site at the 5′ splice site, or that the structural change induced by the pseudouridine may enable specific recognition of branch-site adenosine base substituents during spliceosome assembly.

## MATERIALS AND METHODS

### Design and synthesis of molecular constructs

RNA strands representing the regions of the U2 snRNA and intron involved in the complementary branch-site interaction

were chemically synthesized as short duplexes (sequences shown in Fig. 1C). Oligomers representing the U2 snRNA fragment (GGU GUA GUA and GGU Gd$\psi$A GUA), where d$\psi$ is deoxypseudouridine, were paired with a complementary region of the intron strand (UAC UAA CAC C, where the underlined A corresponds to the branch site). An oligomer without the branch-site A (UAC UAC ACC, which formed an unbulged duplex when paired with the U2 strand) was also synthesized. Oligomers were synthesized trityl-off on a converted ABI model 430A peptide synthesizer using standard phosphoramidite chemistry. RNA oligomers were synthesized on a 5 $\mu$mol scale with commercial phosphoramidites on 500 Å CPG solid support resin (GLEN Research, Sterling, Virginia), using adapted DNA synthesis cycles and 720-s coupling times with 0.05-M RNA phosphoramidite solutions. Oligomers were cleaved from solid support and deprotected according to the manufacturer's protocol and lyophilized to dryness. Triethylamine trihydrofluoride (Sigma) was added to the dried RNA at 1 mL per micromole to desilylate the 2′OH groups. Reactions were quenched after 24 h with 300 $\mu$L of water per micromole and the RNA was precipitated with *n*-butanol (Westman & Stromberg, 1994). The top strand sequence of $\psi$BP (GGU G$\psi$A GUA), purchased from Dharmacon Research, Inc. (Boulder, Colorado), was synthesized using 5′-silyl-2′-orthoester oligonucleotide synthesis chemistry (Meroueh et al., 2000; Scaringe, 2000) and deprotected according to company protocols for ACE chemistry (Scaringe et al., 1998).

RNA oligomers were purified by HPLC using a DNAPac PA-100 semi-prep anion exchange column (Dionex, Inc.), with a 20 mM Tris, pH 8 mobile phase. RNA oligomers were eluted with a 500-mM $NaClO_4$ gradient of 1% per minute. Recovered fractions were concentrated using a stirred-cell apparatus (Amicon, Inc.) with a 1000 MWCO membrane. Concentrated fractions were washed with a high salt buffer (1 M NaCl, 10 mM Na phosphate, 0.1 mM EDTA, pH 6.4) to exchange out residual Tris ions. The samples were then exchanged into a low salt buffer (50 mM NaCl, 10 mM Na phosphate, 0.1 mM EDTA, pH 6.4). Equimolar amounts of top and bottom strands were combined to form duplexes. The samples were dried and resuspended in 90% $H_2O$/10% $^2H_2O$ (Cambridge Isotope Laboratories) for NMR observation of exchangeable protons, or were dried twice from 99.9% $^2H_2O$, once from 99.96% $^2H_2O$, and finally suspended in 99.96% $^2H_2O$ for NMR studies of nonexchangeable protons. Sample concentrations were in the range of 0.8 mM to 1.2 mM at a volume of approximately 250 $\mu$L. Microvolume NMR tubes (Shigemi, Inc.) were used for NMR data collection. $MgCl_2$ (hexahydrate, SigmaUltra) was added to a final concentration of 5 mM in NMR samples of uBP and $\psi$BP. Magnesium was removed by adding 10 mM EDTA to the NMR samples and exchanging into low salt buffer again. Cobaltic hexamine chloride (Acros, Inc.) was then added to a concentration of 5 mM for subsequent studies. The pH of uBP and $\psi$BP was adjusted using 2-$\mu$L aliquots of 0.5 M HCl or 0.5 M NaOH and measuring pH changes with a microelectrode (Ingold, Inc.).

## Thermal denaturation studies

UV absorbance measurements were performed on a Cary 3E spectrophotometer with temperature control using Varian Cary WinUV software. Dry nitrogen gas was flowed through the cell block to prevent condensation below the atmospheric dew point. Temperature was varied from 10 °C to 80 °C at a rate of 1 °C per min, and absorbance measurements at 260 nm were recorded at each integer temperature interval. Samples of 4.5 $\mu$M unbulged duplex, uBP, $\psi$BP, and d$\psi$BP duplexes used for melting studies contained 10 mM Na phosphate, pH 6.4, 0.1 mM EDTA, and 1 M NaCl at a final volume of 250 $\mu$L. One millimeter path-length quartz cuvettes (Hellma, Inc.) were used for data collection. Melting profiles for each of the duplexes were repeated four to six times and found to be reproducible. Thermodynamic parameters were used to calculate theoretical melting temperatures (Freier et al., 1986) for the duplexes. Experimental melting temperatures for the duplexes were calculated from the data using Cary Win UV Thermal data-processing software (Varian, Inc.). Melting curves were fit to a two-state transition curve. $\Delta G^\circ_{37}$ and melting temperatures for each duplex were calculated from van't Hoff thermal parameters, determined from extrapolation of a linear least-squares line fit of the plot $\ln K_T$ versus $1000/T$, where $K_T = 2\alpha/[(1 - \alpha)^2 C_T]$ for a noncomplementary duplex; $\alpha$ = fraction of duplex melted, $n$ = molecularity, and $C_T$ = strand concentration (Puglisi & Tinoco, 1989).

## NMR spectroscopy

All NMR spectra were acquired on a 720-MHz Varian Unity Plus spectrometer (National High Magnetic Field Laboratory, Tallahassee, Florida). Quadrature detection was achieved by implementation of the States method (States et al., 1982) in all experiments, with the exception of the excitation sculpting NOESY experiment (Callihan et al., 1996), for which the States-TPPI method (Marion et al., 1989) was utilized. All NMR data were acquired in the phase-sensitive mode. Two-dimensional experiments were processed using Varian VNMR software, and assigned using SPARKY visualization software. Two-dimensional spectra were apodized with a Gaussian function, and zero-filling was used in both the directly detected and indirectly detected dimensions.

Exchangeable protons were observed at 4 °C with samples in aqueous buffer including 10% $^2H_2O$ to obtain lock. NOESY spectra with 150-ms mixing times were collected using excitation sculpting for solvent signal suppression (Callihan et al., 1996). Spectra were referenced to the residual solvent peak at 5.01 ppm. NOESY spectra acquired for nonexchangeable protons were collected at 20 °C using a low-power irradiation presaturation pulse during the relaxation delay for residual solvent suppression, and were referenced at that temperature to the $H^2HO$ resonance at 4.80 ppm. NOESY spectra were collected at several mixing times to observe buildup and decay of particular NOEs. Sequential assignment from aromatic–anomeric NOEs were made from NOESY spectra collected with 350-ms mixing times. TOCSY spectra utilizing a clean MLEV composite spin lock pulse scheme were collected at 20 °C to identify pyrimidine H5-H6 correlations and strong H1′-H2′ couplings. DQF-COSY spectra, acquired at 20 °C, were collected to identify riboses with C2′-*endo* character based on observable $J_{H1'-H2'}$ couplings. Approximate values for observable H1′-H2′ couplings were measured from one-dimensional traces of DQF-COSY spectra. The accepted values of 1–2 Hz for C3′-*endo* ribose H1′-H2′ couplings and 7–8 Hz for C2′-*endo* were used to assess ribose conformation.

One-dimensional proton-decoupled phosphorous NMR spectra were conducted on a Varian Inova 500 spectrometer (phosphorous frequency 202.3 MHz) at 20 °C and referenced to an external standard of 85% phosphoric acid, $H_3PO_4$ at 0 ppm (3.46 ppm upfield of trimethyl phosphate). All spectra were collected with 2,000 transients. The identical uBP and $\psi$BP NMR samples were used for phosphorous detection as were used for detection of nonexchangeable protons. The NMR sample for the unbulged duplex (ubBP) was prepared identically to the samples for uBP and $\psi$BP.

## ACKNOWLEDGMENTS

We thank Janice Dodge for technical assistance in sample preparation; Hank Henricks and Dr. Umesh Goli of the Florida State University Biochemical Analysis Sequencing and Synthesis Lab for guidance with RNA synthesis; Dr. Joseph Vaughn of the Florida State University Chemistry Department NMR Facility and Dr. Nagarajan Murali of the National High Magnetic Field Laboratory, Tallahassee, Florida, for advice on the collection of NMR spectra; and Dr. Timothy Logan for useful NMR discussions. This project was funded by National Institutes of Health Grant GM54008 to NLG.

*Received November 16, 2000; returned for revision January 5, 2001; revised manuscript received March 29, 2001*

## REFERENCES

Altona C. 1982. Conformational analysis of nucleic acids. Determination of backbone geometry of single-helical RNA and DNA in aqueous solution. *Recl Trav Chim Pays-Bas 101*:413–433.

Arnez J, Steitz T. 1994. Crystal structure of unmodified $tRNA^{Gln}$ complexed with glutaminyl-tRNA synthetase and ATP suggests a possible role for pseudo-uridines in stabilization of RNA structure. *Biochemistry 33*:7560–7567.

Auffinger P, Westhof E. 1998. Effects of pseudouridylation on tRNA hydration and dynamics: A theoretical approach. In: Grosjean H, Benne R, eds. *Modification and editing of RNA.* Washington, DC: ASM Press. pp 103–112.

Bakin A, Lane B, Ofengand J. 1994. Clustering of pseudouridine residues around the peptidyltransferase center of yeast cytoplasmic and mitochondrial ribosomes. *Biochemistry 33*:13475–13483.

Behrens SE, Tyc K, Kastner B, Reichelt J, Lührmann R. 1993. Small nuclear ribonucleoprotein (RNP) U2 contains numerous additional proteins and has a bipartite rnp structure under splicing conditions. *Mol Cell Biol 13*:307–319.

Bevilacqua PC, Turner DH. 1991. Comparison of binding of mixed ribose-deoxyribose analogues of CUCU to a ribozyme and to GGAGAA by equilibrium dialysis: Evidence for ribozyme specific interactions with 2′OH groups. *Biochemistry 30*:10632–10640.

Borer P, Lin Y, Wang S, Roggenbuck M, Gott J, Uhlenbeck O, Pelczer I. 1995. Proton NMR and structural features of a 24-nucleotide RNA hairpin. *Biochemistry 34*:6488–6503.

Callihan D, West J, Kumar S, Schweitzer B, Logan T. 1996. Simple, distortion-free homonuclear spectra of peptides and nucleic acids in water using excitation sculpting. *J Magn Reson B 112*:82–85.

Chu VT, Liu Q, Podar M, Perlman P, Pyle AM. 1998. More than one way to splice an RNA: Branching without a bulge and splicing without branching in group II introns. *RNA 4*:1186–1202.

Davis D. 1995. Stabilization of RNA stacking by pseudouridine. *Nucleic Acids Res 23*:5020–5026.

Davis D, Poulter C. 1991. $^1H$-$^{15}N$ NMR studies of *Escherichia coli* $tRNA^{phe}$ from *hisT* mutants: A structural role for pseudouridine. *Biochemistry 30*:4223–4231.

Durant P, Davis D. 1999. Stabilization of the anticodon stem-loop of the $tRNA^{Lys,3}$ by an $A^+$-C basepair and by pseudouridine. *J Mol Biol 285*:115–131.

Foster P, Huang L, Santi D, Stroud R. 2000. The structural basis for tRNA recognition and pseudouridine formation by pseudouridine synthase I. *Nat Struct Biol 7*:23–27.

Freier S, Kierzek R, Jaeger J, Sugimoto N, Caruthers M, Neilson T, Turner D. 1986. Improved free-energy parameters for predictions of RNA duplex stability. *Biochemistry 83*:9373–9377.

Greenbaum NL, Radhakrishnan I, Hirsh D, Patel DJ. 1995. Determination of the folding topology of the SL1 RNA from *Caenorhabditis elegans* by multidimensional heteronuclear NMR. *J Mol Biol 257*:314–327.

Greenbaum NL, Radhakrishnan I, Patel D, Hirsh D. 1996. Solution structure of the donor site of a *trans*-splicing RNA. *Structure 4*:725–733.

Gu J, Patton J, Shimba S, Reddy R. 1996. Localization of modified nucleotides in *Schizosaccharomyces pombe* spliceosomal small nuclear RNAs: Modified nucleotides are clustered in functionally important regions. *RNA 2*:909–918.

Hall K, McLaughlin L. 1991. Properties of a U1/mRNA 5′ splice site duplex containing pseudouridine as measured by thermodynamic and NMR methods. *Biochemistry 30*:1795–1801.

Hall K, McLaughlin L. 1992. Properties of pseudouridine N1 imino protons located in the major groove of an A-form RNA duplex. *Nucleic Acids Res 20*:1883–1889.

Hermann T, Patel D. 2000. RNA bulges as architectural and recognition motifs. *Structure 8*:1247–1254.

Kieft JS, Tinoco I. 1997. Solution structure of a metal-binding site in the RNA complexed with cobalt (III) hexammine. *Structure 5*:713–721.

Lee C-H, Tinoco I. 1977. Studies of the conformation of modified dinucleoside phosphates containing 1,$N^6$-ethenoadenosine and 2′-*O*-methylcytidine by 360-MHz $^1H$ nuclear magnetic resonance spectroscopy. Investigation of the solution conformations of dinucleoside phosphates. *Biochemistry 16*:5403–5414.

Liu Q, Green JB, Khodadadi A, Haeberli P, Beigelman L, Pyle AM. 1997. Branch site selection in a Group II intron mediated by active recognition of the adenine amino group and steric exclusion of non-adenine functionalities. *J Mol Biol 267*:163–171.

Madhani HD, Guthrie C. 1994. Randomization–selection analysis of snRNAs in vivo: Evidence for a tertiary interaction in the spliceosome. *Genes & Dev 8*:1071–1086.

Marion D, Ikure M, Tschudin R, Bax A. 1989. Rapid recording of 2D NMR spectra without phase cycling. Application to study of hydrogen exchange in proteins. *J Magn Reson 85*:393–399.

Massenet S, Motorin Y, Lafontaine D, Hurt E, Grosjean H, Branlant C. 1999. Pseudouridine mapping in the *Saccharomyces cerevisiae* spliceosomal U small nuclear RNAs (snRNAs) reveals that pseudouridine synthase pus1p exhibits a dual substrate specificity for U2 snRNA and tRNA. *Mol Cell Biol 19*:2142–2154.

McPheeters DS, Abelson J. 1992. Mutational analysis of the yeast U2 snRNA suggests a structural similarity to the catalytic core of group I introns. *Cell 71*:819–831.

Meroueh M, Grohar PJ, Qiu J, Santa Lucia J, Scaringe SA, Chow C. 2000. Unique structural and stabilizing roles for the individual pseudouridine residues in the 1920 region of *Escherichia coli* 23S rRNA. *Nucleic Acids Res 28*:2075–2083.

Moore M, Query C, Sharp P. 1993. Splicing of precursors to mRNA by the spliceosome. In: Gesteland RF, Atkins JF, eds. *The RNA world.* Cold Spring Harbor, New York: Cold Spring Harbor Laboratory Press. pp 303–357.

Nikonowicz E, Gorenstein D. 1990. Two-dimensional $^1H$ and $^{31}P$ NMR spectra and restrained molecular dynamics structure of a mismatched GA decamer oligoribonucleotide duplex. *Biochemistry 29*:8845–8858.

Patel DJ, Hilbers CW. 1975. Proton NMR investigations of fraying in double-stranded d(ATG-CAT) in $H_2O$ solution. *Biochemistry 14*: 2651–2656.

Patton J, Jacobson M, Pederson T. 1994. Pseudouridine formation in U2 small nuclear RNA. *Proc Natl Acad Sci USA 91*:3324–3328.

Portman S, Grimm S, Workman C, Usman N, Egli M. 1996. Crystal structures of an A-form duplex with single-adenosine bulges and a conformational basis for site-specific RNA self-cleavage. *Chem Biol 3*:173–184.

Puglisi J, Tan R, Calnan B, Frankel A, Williamson J. 1992. Conformation of the TAR RNA-Argininamide complex by NMR spectroscopy. *Science 257*:76–80.

Puglisi JD, Tinoco I. 1989. Absorbance melting curves of RNA. *Methods Enzymol 180*:304–325.

Query C, Strobel S, Sharp P. 1996. Three recognition events at the branch-site adenosine. *EMBO J 15*:1392–1402.

Reddy R, Busch H. 1988. Small nuclear RNAs: RNA sequences, structure, and modifications. In: Birnstiel ML, ed. *Structure and function of major and minor small nuclear ribonucleoprotein particles.* Berlin, Germany: Springer-Verlag. pp 1–37.

Saenger W. 1984. *Principles of nucleic acid structure.* New York: Springer-Verlag.

Scaringe SA. 2000. Advanced 5′-silyl-2′-orthoester approach to RNA oligonucleotide synthesis. *Methods Enzymol 317*:3–18.

Scaringe SA, Wincott FE, Caruthers MH. 1998. Novel RNA synthesis method using 5′-*O*-silyl-2′-*O*-orthoester protecting groups. *J Am Chem Soc 120*:11820–11821.

Smith J, Nikonowicz E. 1998. NMR structure and dynamics of an RNA motif common to the spliceosome branch-point helix and the RNA-binding site for phage GA coat protein. *Biochemistry 37*: 13486–13498.

States DJ, Haberkorn RA, Ruben DJ. 1982. A two-dimensional nuclear Overhauser experiment with pure absorption phase in four quadrants. *J Magn Reson 48*:286–292.

Thiviyanathan V, Guliaev AB, Leontis NB, Gorenstein DG. 2000. Solution conformation of a bulged adenosine base in an RNA duplex by relaxation matrix refinement. *J Mol Biol 300*:1143–1154.

Varani L, Hasegawa M, Spillantini MG, Smith MJ, Murrell JR, Ghetti B, Klug A, Goedert M, Varani G. 1999. Structure of tau exon 10 splicing regulatory element RNA and destabilization by mutations of frontotemporal dementia and parkinsonism linked to chromosome 17. *Proc Natl Acad Sci USA 96*:8229–8234.

Westman E, Stromberg R. 1994. Removal of *t*-butyldimethylsilyl protection in RNA synthesis. Triethylamine trihydrofluoride (TEA, 3HF) is a more reliable alternative to tetrabutylammonium fluoride (TBAF). *Nucleic Acids Res 22*:2430–2431.

Wijmenga S, Mooren M, Hilbers C. 1993. NMR of nucleic acids; from spectrum to structure. In: Roberts GCK, ed. *NMR of macromolecules: A practical approach*. Oxford: Oxford University Press. pp 217–288.

Wu J, Manley JL. 1989. Mammalian pre-mRNA branch site selection by U2 snRNP involves base pairing. *Genes & Dev 3*:1553–1561.

Yarian C, Basti M, Cain R, Ansari G, Guenther R, Sochacka E, Czerwinska G, Malkiewicz A, Agris P. 1999. Structural and functional roles of the N1- and N3-protons of Ψ at tRNA's position 39. *Nucleic Acids Res 27*:3543–3549.

Yu YT, Shu MD, Steitz JA. 1998. Modifications of U2 snRNA are required for snRNP assembly and pre-mRNA splicing. *EMBO J 17*:5783–5795.